Effect of Floor Slab on Behavior of Slab-Beam-Column Connections

by C.W. French and J.P. Moehle

Synopsis: In structures subjected to lateral loading, slab reinforcement acting as effective tensile reinforcement of the beams has been found to significantly increase the beam flexural strength. The enhanced beam flexural strength has several effects on the structural behavior including a shift in the ratio of strengths between the beams and other members. This may result in a failure mechanism different from that anticipated. The slab contribution depends on several variables including the connection type (interior or exterior), lateral deformation level, and lateral load history (uniaxial or multiaxial). This paper summarizes general behavior observed during isolated and multiple beam-column-slab connection tests. An approximation is given for estimating the amount of slab reinforcement to be considered as effective tensile reinforcement of the beams.

Keywords: Beams (supports); columns (supports); earthquake-resistant structures; flexural strength; joints (junctions); loads (forces); reinforced concrete; slabs; T beams; tests

Catherine W. French is an Associate Professor in the Department of Civil and Mineral Engineering at the University of Minnesota, Minneapolis. She is a member of ACI Committees 368 - Earthquake Resisting Elements and Systems, 352 - Monolithic Joints and Connections, and 423 - Prestressed Concrete.

Jack P. Moehle is Professor of Civil Engineering at the University of California at Berkeley. He is member of ACI Committees 318 sub H, 352, 408, and 442, and chairman of ACI Committee 368, Proportion and Detail of Earthquake Resisting Elements and Systems.

INTRODUCTION

In 1981, pseudodynamic tests were conducted on a model of a seven-story reinforced concrete frame-wall building at the Building Research Institute (BRI) in Tsukuba, Japan [1]. Using conventional modeling assumptions, the base shear strength of the structure was calculated to be approximately 60% of the measured strength. The discrepancy between the calculated and measured strengths was attributed to the unexpected contribution of the floor slab reinforcement to the flexural tensile strength of the longitudinal beams, and to a lesser extent, three-dimensional effects created by rocking of the wall. In acting as tension reinforcement for the beams in flexure, the slab reinforcement increased the beam flexural strength and the entire building strength to values well in excess of the expected strengths.

Ignoring the floor slab contribution to design flexural strength may be conservative in some situations because it results in an underestimation of the structural base shear strength. However, it may also result in unexpectedly high accelerations and inertial forces, as well as a shift in the ratio of strengths between beams and other members. The consequence may be development of a failure mechanism different from that which is anticipated.

Current U.S. design codes [2] and recommendations [3] do not provide guidance for the effective width of slab to be considered as flexural reinforcement for beams subjected to lateral loading. Provisions of those documents are based largely on test results of subassemblages comprising columns and beams without floor slabs. Until recently there has been little information available on the effect of slab on beam flexural strength.

The floor slab contribution to lateral resistance observed in the BRI test inspired much interest among researchers. Some of the research that has been conducted to date related to slab participation in resisting lateral load is presented. The discussion is focussed on results of several laboratory experiments m-column-slab subassemblages and complete frames subjected teral load. In addition, some analytical models of olumn-slab connections are described.

DESCRIPTION OF TESTS

The following is a brief description of several of the atory experiments on monolithic beam-column-slab systems.

lated Connection Tests

A schematic view of a typical beam-column-slab test subassemblage is shown in Fig. 1. Members of the subassemblage span to assumed inflection points located at member midspans in the prototypes. In a test, lateral loading is simulated either by loading the columns or the beams; gravity load effects are simulated in some cases. Details particular to several tests on isolated connections of the type shown in Fig. 1 are given in Tables 1 and 2 for interior and exterior connections, respectively. Brief descriptions of the tests follow.

As part of the U.S.-Japan cooperative research program on the seven-story reinforced concrete frame-wall structure, four subassemblages were tested at the University of Texas at Austin [4,5]. The models incorporated edge beams (not shown in Fig. 1) at the assumed inflection points (that is, at the slab perimeter in the subassemblages). In another research program, interior subassemblages were tested biaxially along a line oriented 45 degrees from the frame lines [6]. The corners of the slabs were coped in the biaxially-loaded specimens to accommodate placement in the loading frame.

One-half scale models of interior connections were tested unidirectionally at the University of Tokyo [7,8] and the University of Minnesota [9,10]. Corners of the slab were coped to fit the testing apparatus in the University of Tokyo model. The depth of the transverse beam element was varied among the University of Minnesota models to determine the influence of the transverse beam stiffness on slab participation.

At the University of Michigan, unidirectional tests were conducted on three interior connections [11] and six exterior connections [12]. All specimens had transverse beams. The primary variables in these tests included: ratio of column to beam flexural strength, amount of joint transverse reinforcement, and joint shear stress.

Zerbe and Durrani [13] tested four unidirectionally-loaded exterior connections in which the width of slab was varied. All four of these specimens had transverse beams. The objectives of the tests were to determine the effect of the slab on joint confinement provided by the transverse beams and to estimate the effective slab width.

In addition to these tests, the US-NZ-Japan-China Cooperative Research Program on Reinforced Concrete Beam-Column Joints has provided a wealth of information on beam-column-slab behavior. Under the auspices of this program, one exterior and two interior specimens were loaded biaxially along the frame lines at the University of Texas at Austin [14,15]. One of the interior specimens did not contain transverse beams. The corners of the slab were coped in all cases. In New Zealand, one exterior and two interior connections were tested [16-18]. One interior specimen did not contain transverse beams and was subjected to unidirectional loading. One exterior and two interior subassemblages were also tested at the University of Tokyo [19,20]. All of the specimens had transverse beams, slab corners coped, and unidirectional loading. At Kyoto University, five exterior subassemblages with both transverse and edge beams were subjected to bidirectional loading [20]. Bidirectional tests were conducted on interior and exterior connections with transverse beams and slab corners coped at Beijing [21] and Tongji [22] Universities in China, respectively.

Multiple Connection Tests

A quarter-scale model of a six-story beam-column-slab frame system has been tested on the shake table of the Earthquake Engineering Research Center [23] at the University of California at Berkeley. The model had two bays by two bays in the lower three stories, reducing to one bay by two bays above the third story. It was subjected to uniaxial base motions parallel and skew to the principal axes of the frames. A quarter-scale two-bay subassemblage of this system was subsequently tested [24,25]. The columns in the subassemblage extended from footings to assumed inflection points at midheight of the second story (Fig. 2). The slab and columns were loaded to simulate gravity load effects. Lateral loads were applied at tops of the columns.

The BRI seven-story frame-wall structure described previously may also be included in the group of indeterminate beam-column-slab test structures. The structure had three bays parallel to the direction of lateral loading and two in the transverse direction. The central bay of the central frame had a structural wall oriented parallel to the direction of lateral load.

OBSERVATIONS FROM THE TESTS

The slab has the greatest effect on the flexural strength of beams bent in negative curvature (top of beam in tension). Consequently, this behavior is emphasized in this section.

General Aspects of Behavior

In beam-column-slab elements subjected to lateral loading, tensile strains develop in the reinforcement across the slab bent in negative curvature. As indicated by reinforcement strain measurements shown in Fig. 3 [15], the slab tension tends to be largest near the longitudinal beam, and decreases with increasing distance from the longitudinal beam. The slab tensile strains generally increase with increasing deformation of the connection; at large lateral deformations, slab reinforcement strain may exceed the yield strain across the entire slab width. A typical illustration of this behavior is presented in Fig. 4 for Specimen EW3 reported by French et al. [9,10,26,27].

Although experiments [9,15] indicate some variation of slab strain through the depth, the variation near the column is small relative to the total magnitude of strain developed. For the tests examined, the slab acts primarily as a membrane element, without development of appreciable flexural moment within the slab itself.

The tensile forces that develop across the slab have a significant impact on the flexural capacity of the beam. A free-body diagram cut perpendicular to the longitudinal beam at a location near the column exposes internal tension forces in reinforcement both of the beam web and of the slab balanced by compression in the bottom of the beam (Fig. 5). Thus, the total effective tensile reinforcement of the beam is equal to the area of beam tension reinforcement plus a portion of the slab reinforcement.

The participation of the slab as a tensile element of the beam is evident visually in crack patterns in the test specimens. Flexural cracks develop in the upper portion of the beam and spread transversely in the slab. The crack pattern shown in Fig. 6 [15] illustrates the extent of cracking possible after severe lateral deformations have been imposed.

The mechanism by which the connection develops slab tension has been indicated by Kurose, et al. [20], Cheung, et al. [16-18], and Pantazopoulou, et al. [28,29]. The action of the slab is initiated by flexural deformations of the longitudinal beam. As the beam is subjected to negative bending moment, the top surface of the beam elongates along the beam length. The elongation is transferred through in-plane shear to the slab. The accumulation of shear along the length of the longitudinal beam results in slab tension that must be transmitted through membrane action to a section of the slab located at the interface of the transverse beam and the slab (Fig. 7). The slab tension forces acting along the length of the transverse beam (shown in Fig. 7) are those identified in experiments such as shown in Figs. 3 and 4.

In addition to slab tension along the transverse beam, moment equilibrium of the isolated subassemblage slab panel bounded by longitudinal and transverse beams requires that transverse slab tension forces also develop along the longitudinal beam (Fig. 8). Fig. 9 shows the transverse slab reinforcement strains which were measured along the longitudinal beam of EW3 [9,10]. Furthermore, force equilibrium requires slab shear stresses along the interface between the slab and transverse beam.

Effect of Connection Geometry

The tensile forces developed across the slab must be equilibrated by equal and opposite forces across the section (Fig. 10). Some of these forces are transmitted to the column through shear, flexure, and torsion of the transverse beam. In the case of exterior connections, the action of the transverse beam is the only means to resist these tensile forces in the slab. Consequently, the stiffness of the transverse beam has an important effect on slab participation in exterior connections. The transverse beam will twist and flex under the action of the slab, thereby relieving the tendency for slab tensions to develop. In tests reported by Kurose [15], the spandrel beam was apparently capable of developing the full slab tensile strength. In other tests, spandrel beams were relatively weaker and failed in torsion so that less slab contribution developed [13,24].

In the case of an interior connection, tensile forces that develop on the side of the slab bent in negative curvature are transferred both to the transverse beam and to the slab on the opposite side of the transverse beam (Fig. 10). Tensile forces developed across the slab bent in negative curvature tend to deflect the transverse beam in weak-axis bending and torsion. This action appears to generate tensile forces between the transverse beam and the relatively stiff slab panel on the positive curvature side. Thus, the slab is usually in tension on both sides of the column. Because of this action, the role of the transverse beam is reduced for interior connections. In many of the reported tests, damage to the transverse beam was light; however, some torsional distress was observed in tests by several researchers [4,9-10,24]. Tests reported by Boroojerdi and French [9-10] and Kurose [15] indicate that an increase in transverse beam cross section tends to promote greater slab participation at earlier drift levels (Fig. 4).

Because most connections tested to date have been configured to represent typical proportions, there is not a wide variation in the geometry of the test specimens (Tables 1 and 2). Thus, effects on slab participation of geometric variables such as beam size and slab aspect ratio cannot be determined directly from available data.

Effect of Biaxial Loading

Most of the tests discussed above involved load along one horizontal axis. To account for damage caused by earthquake loading in other directions, some of the subassemblages were tested biaxially [6-10,14,15,20].

In the biaxial tests reported by Guimaraes et al. [14,15], the connections were able to achieve approximately 80% of the full slab width participation at drifts of approximately 4%. However, there were no uniaxial tests conducted on similar specimens, so the influence of biaxial loading is not known. Suzuki et al. [7,8,20] compared the results of a subassemblage tested uniaxially with the results of a similar model tested biaxially. The main difference observed between the bidirectional and uniaxial results was that the bidirectional lateral load reversals applied to the column resulted in larger deflections.

Boroojerdi and French [9,10] included tests on a connection loaded first in one direction to modest deformation levels, and then loaded in the opposite direction. The tests indicated that previous damage due to loading in the transverse direction initially decreased the resistance and stiffness of the connection in comparison with one loaded only uniaxially. The effect became negligible as the connection was displaced beyond the maximum deformation level imposed in the first direction.

In tests reported by Cheung, et al. [16-18], the uniaxially-loaded specimen achieved yielding across the entire slab at a displacement ductility of two (1% drift); in the case of the bidirectionally-loaded model, full yielding was achieved at a displacement ductility of four (2% drift). As reported by Suzuki, et al. [7,8,20], the increased drift for biaxially-loaded connections may be partially attributed to increased column flexibility under biaxial loading.

Effect of Boundary Conditions

In isolated subassemblages the boundary conditions differ from those that occur in actual structures with regards to several aspects, including locations of inflection points, coped slab corners, and free slab boundaries around the perimeter of the subassemblage. This latter difference is believed to be particularly significant, and is detailed below, considering slab shear deformations, flexural deformations, and rigid-body rotations.

The effect of slab shear deformations is illustrated in Fig. 11. As discussed previously, in an isolated interior connection test the slab reinforcement is in tension on both sides of the column (Fig. 10). These tensions are equilibrated in part by slab shear stresses along the longitudinal beam. The resulting slab shear distortions are thus of opposite sign on opposite sides of the longitudinal beam, and opposite sides of the transverse beam (Fig. 11). In a continuous structure these distortions are not possible because they would result in a discontinuity in the slab at the midspan. Thus, the slab shear must be modified in a continuous structure. Because the shear distortion accounts partially for the reduction in effectiveness of slab reinforcement across the slab width [26,27] the mechanism of slab contribution must differ in isolated and continuous connections.

Slab flexural deformations may also differ in isolated and continuous connections. In a typical isolated connection test, the longitudinal beam is restrained at both ends and the slab perimeter is unrestrained. As a consequence, when lateral load is applied the "free" edges of the slab tend to deflect vertically relative to the longitudinal beam (Fig. 12). The resulting slab deformations at opposite ends of the slab panel would result in a discontinuity in a continuous slab. The added restraint in a continuous structure will enforce a more uniform slab contribution.

A third effect of boundary conditions is illustrated in Fig. 8. In an isolated connection, the slab tension forces that develop along the interface with the transverse beam must be equilibrated partially by transverse slab tension forces at the interface with the longitudinal beam. The slab tension stresses cause rigid body rotation of the slab about a vertical axis away from the longitudinal beam. The rigid body rotation is evident in strain distributions (Fig. 9) and from cracks that typically open between the slab and the longitudinal beam. This rotation results in deformation of the slab boundaries that would be incompatible in a continuous structure. To develop compatibility, the rotation must be reduced, and a more uniform slab strain distribution would result.

The preceding discussion leads to the conclusion that slab action in a continuous structure differs from that in an isolated connection. The difference is immediately apparent by comparison of crack patterns that develop in a slab in continuous and isolated connections (Fig. 13). The difference has also been apparent in transverse slab strains. In the seven-story frame-wall structure tested at BRI [30], the transverse slab strains were maximum at the column and decreased toward the longitudinal beam midspan (Fig. 14), whereas the opposite trend was observed in isolated connection tests (Fig. 9). However, longitudinal slab strains, have been observed to reduce with increasing distance from the longitudinal beam in much the same manner as for isolated connections (Figs 3,4,14). The overall effect of increased restraint in continuous structures may be that the slab contribution is larger in such structures as compared with results from isolated connection tests. However, further study is required before definite conclusions on this subject may be drawn.

MODELING BEAM-SLAB BEHAVIOR

Cheung et al. [17] used the truss analogy to describe the avior of a beam-column-slab subassemblage. This model explains development of orthogonal tensile forces in the slab, and the esponding diagonal compression field corresponds reasonably with observed crack inclinations at late stages of testing of of the isolated connections. As discussed in the preceding ion, the boundary conditions and apparent crack patterns in inuous frames differ from those of isolated connections. The s analogy as proposed by Cheung et al. may require modification t is to be applied to continuous structures.

Pantazopoulou et al. [28] proposed a procedure to determine effective slab width using a model that approximated the linear strain distribution across the slab. Based on the assumed pe function, it was possible to derive an expression for the fective slab width based on the reinforcement properties, the imum strain in the beam, and the maximum slab width. This model s developed for connections with an effectively rigid transverse beam element, and is thus not applicable to typical exterior connections. Pantazopoulou has developed an alternate model for interior connections [29] and a three-dimensional truss model [25] for exterior connections.

A MEASURE OF THE SLAB CONTRIBUTION

To gage the effect of the slab on flexural strength of slab-beam-column connections, data from available experiments (Tables 1 and 2) were evaluated. In the evaluation, measured beam flexural strengths were compared with those calculated for assumed effective slab widths. A recommendation for effective width is made based on results of the comparison.

It has been shown in previous sections that the slab participation in resistance to lateral loads is a complicated function of several parameters including the magnitude of lateral deformation, shear deformation and rigid body rotation of the slab, material properties, and stiffness of the transverse beam element. With respect to the first parameter, it has been shown from the tests that if a structure is displaced sufficiently far, the entire slab width may participate as a tension flange of the longitudinal beam. In some tests, EW1 for example [9,10], this was not achieved until story drifts (ratio of lateral story displacement to story height) exceeded 7%. It is not reasonable to expect that this amount of participation would be realized in an earthquake because second-order effects would precipitate failure at an earlier drift.

In a judicious design, lateral drifts are likely to be restricted to values well below those at which full slab participation would be observed [31]. A level of 2% drift was selected here to represent a reasonable upper limit for a well-designed building subjected to strong ground motion. Other measures of deformation are possible but not considered here.

Measured Strengths

The measured flexural strengths of the beams bent in negative curvature were determined from the tests listed in Tables 1 and 2 at an interstory drift of 2%. The moment resistance of the beams as a function of deformation level was determined directly from the original reports on the slab-beam-column subassemblage tests. For interior connections, beam moments were determined from the reported beam shear (or moment) history and geometry. For exterior connections, it was possible to resolve the beam moment history from the reported total specimen load-deformation history and geometry. Measured strengths at 2% drift ($M_{0.02}$) are given in Tables 1 and 2.

Calculated Strengths

Beam flexural strengths were calculated for each of the beams listed in Table 2 using reported dimensions and material properties. In the calculation, plane sections were assumed to remain plane. Concrete compression stresses were represented using the rectangular stress block and maximum concrete compression strain of 0.003 as specified in the ACI Building Code [2]. Steel in compression and tension was assumed to have an elasto-plastic stress-strain relation with an effective yield stress equal to 1.25 times the measured tensile yield stress. The factor 1.25 was selected to account for effects of strain hardening, and was based on calculations of expected plastic hinge rotational requirements for a typical frame with typical Grade 60 steel undergoing 2% lateral interstory drift [32].

The slab steel within an assumed effective width was taken to be fully effective in resisting beam negative moments. The effective width is defined here as the total width including the beam web width plus an overhanging portion of slab on each side of the web. In calculating the beam flexural strengths, a linear strain distribution (plane sections remain plane) was assumed across the entire effective cross section. Slab reinforcement outside the effective width was ignored.

Three slab effective widths were investigated: (1) The beam web width (web), (2) the ACI effective width (ACI), and (3) a width equal to the beam web width plus three times the longitudinal beam depth (b_w+3h). The intent of the ACI effective width criterion is to prescribe the width of slab to be considered as a compression flange to the beam (top of beam in compression) [2]. In this paper, it is used to estimate the amount of slab reinforcement which acts as additional tensile reinforcement of the beam (top of beam in tension). The ACI effective width is defined as the least of (a) the web width plus 16 slab thicknesses, (b) the transverse dimension of the subassemblage, and (c) one-quarter of the longitudinal dimension of the subassemblage [2]. In most cases, the last of the three criteria controlled the ACI effective width. The width equal to the beam web width plus three times the longitudinal beam depth has been proposed by Pantazopoulou, et al. [28]. The ACI effective width and the effective width proposed by Pantazopoulou, et al. are similar for the connections considered in this study. Calculated flexural strengths (M_{web}, M_{ACI}, M_{bw+3h}) are listed in Tables 1 and 2.

Comparison of Measured and Calculated Strengths

Ratios of calculated to measured strengths at 2% drift (M_{calc} / $M_{0.02}$) for the various specimens are presented in Fig. 15. Note that specimens 1 through 13 represent interior connections and the remainder, 21 through 27, represent exterior connections.

The comparison between measured and calculated beam negative moment strengths (Fig. 15) indicates that the strength calculated based on the web steel alone can significantly underestimate the moment resisted by the connections at a lateral drift of 2% of height. Only in cases where the slab reinforcement was light relative to the web longitudinal steel, and the strength therefore could not be significantly influenced by the slab contribution, was the strength based on the web alone close to the actual resistance (eg., connections 5 through 9 in Fig. 15). Strengths calculated using either the ACI or b_w+3h slab effective width assumptions were in general much closer to the measured resistances. Either of these two assumptions appears to provide a simple means to estimate the slab participation at 2% drift assuming an amplified yield stress of 1.25 times the measured value for the subassemblages investigated which had a relatively narrow range of geometric variables. It must also be emphasized that the assumed tensile stress has a significant effect on the results. A lower assumed reinforcement tensile stress would require a larger effective slab width (more steel area) to produce the same calculated flexural strengths as those given with the current tensile stress assumption.

From the data in Tables 1 and 2, it can be determined that strengths calculated considering the web alone are on average 25% and 17% below strengths measured for interior and exterior connections, respectively. Thus, the slab participation is on the average lower for the exterior connections. The lower slab participation occurs because slab membrane action cannot develop perpendicular to the free edge of an exterior connection to the same extent that is possible for an interior connection. As discussed previously, the slab participation for an exterior connection is limited by the stiffness and strength of the spandrel beam. It should also be noted that Table 2 and Fig. 15 contain data only for connections in which failure of the transverse beam was not observed. If beam failure occurs, as is possible for exterior connections, slab contributions are likely to be reduced.

Discussion in the preceding paragraphs suggests that the slab effective widths as defined in this paper are indeed crude approximations. In a more refined definition, variables other than or in addition to those considered here should be included. For exterior connections in particular, the effective width is a function of the transverse beam stiffness. Resistances of interior connections EW1, EW2, and EW3, measured at particular drift levels, also varied apparently as a function of the transverse beam stiffness (Table 1). This indicates that transverse beam stiffness is a relevant variable for interior connections as well. Load history also has a marked influence on the slab contribution, as evinced by the different resistances of specimens subjected to uniaxial and biaxial loading [15,18,20]. Although it is clear that the slab effective width as defined in this paper is a simple approximation, further refinement is unwarranted given the limitations of the available data.

EFFECT OF SLAB CONTRIBUTION ON STRUCTURAL BEHAVIOR

Previous discussions have demonstrated that the slab can influence significantly the flexural behavior of the longitudinal beams. The significance of this action to structural behavior and design is broad. Several effects of this action are summarized below.

<u>Structure strength and stiffness</u>--Increasing the flexural strength and stiffness of the beams may result in enhanced lateral load resistance for the entire structure. The enhanced strength and stiffness will improve the service level lateral load behavior of the frame. For some structures, particularly shorter period structures, the enhanced strength may result in reduced overall deformation and ductility demands. Because of increased stiffness, reduced lateral deformations may be likely for longer period structures as well. A disadvantage of the increased flexural strength is that the increased base shear resulting from neglected slab participation may result in unexpectedly high accelerations and forces in the structure. It may create shear distress or other undesirable damage patterns in the system by generating more force than expected.

<u>Beam behavior</u>--Acting as a tension flange to the beams, the slab will produce increased flexural compression forces in the compression zones of the beam. Thus, the composite action will result in reduced flexural deformability of the beam. Also, assuming the formation of flexural hinges at beam ends, the

enhanced beam flexural strength will induce greater shear in the beams. Because the increased shear is resisted primarily by the web, further reductions in beam deformability are likely. Furthermore, by increasing the negative bending resistance of the beam more than the positive bending resistance, under lateral loading the moment distribution along the span may be different than expected without the slab. In extreme situations, flexural tension may extend beyond bar cutoffs that were intended to be in regions of compression. Such shifts in inflection points have not been observed in isolated connection tests because the inflection points are maintained at midspan throughout the tests.

<u>Joint behavior</u>--The slab contribution to flexural resistance of the longitudinal beam manifests itself in increased joint shear. Obviously, the increased flexural compression force acting at the bottom of the longitudinal beam subjected to negative bending will be transferred directly to the joint. Based on the pattern of slab strains, Cheung et al. [17,18] have hypothesized that the slab tension is equilibrated primarily by concrete compression struts that react at the back face of the joint at the level of the slab (Fig. 10). Thus, in interior joints, according to this hypothesis the increased joint shear force is applied directly along the compression zone of the longitudinal beams and is resisted within the joint by an inclined compression strut. For this reason, additional joint "shear reinforcement" may not be necessary. However, it is conceivable that the increased force acting along the main diagonal compression strut will induce failure of this strut; therefore it may be necessary to account for the enhancement of beam strength when considering joint design. In exterior joints, the increased tensile force provided by the slab reinforcement is introduced to the joint through shear, weak-axis bending and twist of the transverse beam. These actions may require placement of additional shear reinforcement within the joint.

Another aspect related to joint behavior is the effect of the slab contribution on bond. The large reversals of compression and tension forces in the beam reinforcement tend to cause bond deterioration. Although this deterioration seems equally likely for both the top and bottom beam reinforcement through the joint, it was noted only in bottom reinforcement in tests by Durrani and Wight [11], Guimaraes et al. [14,15], and Qi [24].

<u>Column and overall frame behavior</u>--Because the beam flexural strength is enhanced, the demand on the columns will be increased during severe ground shaking. From the experimental data, it is reasonable to expect that the sum of actual beam strengths may be as much as 1.5 times the values computed according to conventional beam theory ignoring the slab contribution. Thus, the design ratios between column and beam strengths as specified in ACI 352-85 [3] may be insufficient to prevent column hinging. However, because the slab contribution to flexural strength may not fully develop until large deformations are imposed, and because the need to avoid column hinging in an otherwise robust frame has not been conclusively proven [33], the significance of beam overstrength as

it relates to column hinging and overall frame behavior should not be automatically assumed.

CONCLUSIONS

The slab action in beam-column-slab systems is a complex phenomenon that depends on a wide range of variables. The main action of the slab identified here is its participation as a tensile element that adds to the flexural resistance of the longitudinal beams when the top of the beam is in tension. The slab contribution to the beam resistance depends on several variables including connection type (interior or exterior), transverse beam stiffness, lateral deformation level, and lateral load history (uniaxial or multiaxial). At present there appear to be no analytical solutions for this action that account properly for all pertinent variables.

For design, a simple means of accounting for the slab contribution to the beam flexural strength (top of beam in tension) is to assume that all slab reinforcement within a slab effective width acts as beam tension reinforcement. An analysis of available test data indicates that if the slab effective width is taken equal to the ACI effective width, calculated flexural strength will approximate measured beam resistance for frame lateral drift equal to 2% of height. To account for effects of reinforcement strain hardening in the strength calculation, the effective reinforcement yield stress should be taken not less than 1.25 times the actual yield stress. The actual yield stress may be higher than the nominal value, and this difference should be considered.

In acting with the beam as a tension flange, the slab affects other actions within a beam-column-slab frame. The enhanced beam flexural strength may result in increased beam shear that should be considered in selecting transverse reinforcement. Shifts in beam moment distributions are likely; these should be considered in selecting longitudinal reinforcement details including bar cutoffs. Demands on beam-column connections are also increased. Additional joint shear reinforcement for exterior connections and increased joint sizes for all connections can be rationalized given the increased demand, but at present there is no hard evidence demonstrating these needs. Finally, the slab contribution should be considered in determining required column strengths to avoid excessive column hinging in frames subject to severe lateral loading.

ACKNOWLEDGMENTS

The work described here was influenced significantly by research carried out at the University of Minnesota and the University of California at Berkeley, as well as by research discussions at workshops related to the US-NZ-Japan-China Cooperative Research Program on Reinforced Concrete Beam-Column Joints. The National Science Foundation of the United States provided funding for these activities. Statements made in the paper represent those of the authors, and do not necessarily reflect those of the NSF or of other participants in the US-NZ-Japan-China Cooperative Research Program.

NOTATION

$l1$	-	slab span in longitudinal direction
$l2$	-	slab span in transverse direction
b_w	-	longitudinal beam width
h	-	longitudinal beam depth
b_{trans}	-	transverse beam width
h_{trans}	-	transverse beam depth
t_f	-	slab thickness
A_s	-	area of top steel within beam web
A_s'	-	area of bottom steel within beam web
A_{s1}''	-	area of slab steel within width b1 nearest the beam web
A_{s2}''	-	area of slab steel within width b2 farthest from the beam web
b_1	-	width of slab nearest the beam web containing slab reinforcement A_{s1}''
b_2	-	width of slab farthest from beam web containing slab reinforcement A_{s2}''
d	-	effective depth of reinforcement A_s from extreme compression fiber
d'	-	effective depth of reinforcement A_s' from extreme compression fiber
d''	-	average effective depth of reinforcement A_s'' from extreme compression fiber
f_y	-	reported yield strength of reinforcement A_s
f_y'	-	reported yield strength of reinforcement A_s'
f_y''	-	reported yield strength of reinforcement A_s''
f'_c	-	reported concrete compressive strength
$M_{0.02}$	-	beam flexural strength measured at 2% interstory drift
M_{web}	-	calculated flexural strength assuming effective flange width = b_w
M_{ACI}	-	calculated flexural strength assuming ACI effective flange width
M_{web+3h}	-	calculated flexural strength assuming effective flange width = b_w+3h

Refer to Fig. 1 for further description of notation.

REFERENCES

1. U.S.-Japan Research: Seismic Design Implications. (JTCC1988). (1988). Joint Tech. Coordinating. Comm., J. of Struc. Engrg., ASCE, 114(9), 2000-2016.

2. Building Code Requirements for Reinforced Concrete. (ACI 318-89). (1989). Amer. Concr. Inst., ACI Comm. 318, Detroit, Mich.

3. Recommendations for Design of Beam-Column Joints in Monolithic Reinforced Concrete Structures. (ACI 352-85R). (1985). Amer. Concr. Inst., ACI-ASCE Comm. 352, Detroit, Mich., ACI J., 82(3), 266-284.

4. Joglekar, M. R. (1984) "Behavior of Reinforced Concrete Floor Slabs under Lateral Loads," Doctoral Dissertation, Graduate School, University of Texas at Austin, 210 pp.

5. Joglekar, M. R., Murray, P. A., Jirsa, J. O. and Klingner, R. E. (1985). "Full Scale Tests of Beam-Column Joints," ACI SP 84-10, Earthquake Effects on RC Structures: U.S. Japan Research, ACI SP 84-10, 271-304.

6. Leon, R. T. (1983) "The Influence of Floor Members on the Behavior of Reinforced Concrete Beam-Column Joints Subjected to Severe Cyclic Loading," Doctoral Dissertation, Graduate School, University of Texas at Austin, 422 pp.

7. Suzuki, N., Otani, S. and Kobayashi, H. (1984) "Three-Dimensional Beam-Column Subassemblages under Bidirectional Earthquake Loadings," Proceedings, Eighth World Conference on Eqke. Engrg., v.6, San Francisco, 453-460.

8. Suzuki, N. Otani, S. and Aoyama, H. (1983) "The Effective Width of Slabs in Reinforced Concrete Structures," Trans. of Japan Concr. Inst., 5(V-6-B), Dept. of Arch., Faculty of Engrg., University of Tokyo, Japan., 154-161.

9. Boroojerdi, A. and French, C. W. (1987) "T-Beam Effect in Reinforced Concrete Structures Subjected to Lateral Load," Struc. Engrg. Report No. 87-04, Dept. of Civ. and Min. Engrg., University of Minnesota, 300 pp.

10. French, C. W. and Boroojerdi, A. (1989) "Contribution of R/C Floor Slabs in Resisting Lateral Loads," J. Struc. Engrg., ASCE, 115(1), 1-18.

11. Durrani, A. and Wight, J. K. (1987) "Earthquake Resistance of Connections Including Slabs," Struct. J., ACI, 84(5), 400-406.

12. Ehsani, M. and Wight, J. K. (1985) "Effect of Transverse

Beams and Slab on Beam-to-Column Connections," J. Am. Concr. Inst., 2(82), 188-195.

13. Zerbe, H. E. and Durrani, A. J. (1985) "Effect of a Slab on the Behavior of Exterior Beam to Column Connections," Struct. Res. at Rice Report No. 30, Dept. of Civ. Engrg., Rice University, Houston, TX, 159 pp.

14. Guimaraes, G. N., Kurose, Y., Liu, Z., Kreger, M. E. and Jirsa, J. O. (1987) "Tests of Reinforced Concrete Slab-Beam-Column Connections - U.S. Designs," Interim Rep., University of Texas at Austin, Prepared for US-NZ-Japan-China Seminar on Design of RC Beam-Column Joints for Earthquake Resistance, University of Canterbury, Christchurch, NZ, 10-12 August 1987.

15. Kurose, Y., Guimaraes, G., Liu, Z., Kreger, M. and Jirsa, J. (1988) "Study of Reinforced Concrete Beam-Column Joints under Uniaxial and Biaxial Loading," PMFSEL Rept. No. 88-2, Phil M. Ferguson Structural Engineering Laboratory, Univ. of Texas, Austin, 146 pp.

16. Paulay, T. and Park, R. (1984) "Joints in Reinforced Concrete Frames Designed for Earthquake Resistance," Res. Rep. No. 84-9, Dept. of Civ. Engrg., University of Canterbury, Christchurch, NZ, 35-36.

17. Cheung, P., Paulay, T. and Park R. (1987) "A Reinforced Concrete Beam-Column Joint of a Prototype One-Way Frame with Floor Slab Designed for Earthquake Resistance," Res. Rep. No. 87-6, Dept. of Civ. Engrg., University of Canterbury, Christchurch, NZ, 44-51.

18. Cheung, P., Paulay, T. and Park, R. (1989) "Interior and Exterior Reinforced Concrete Beam-Column Joints of a Prototype Two-Way Frame with Floor Slab Designed for Earthquake Resistance," Rept. No. 89-2, Dept. of Civ. Engrg., University of Canterbury, Christchurch, NZ, 80 pp.

19. Kitayama, K., Otani, S. and Aoyama, H. (1988) "Behavior of Reinforced Concrete Beam-Column-Slab Subassemblages Subjected to Bi-Directional Load Reversals," Proc. Ninth World Conf. on Eqke. Engrg., Tokyo-Kyoto Japan, Paper No. SF-10, Vol. VIII, VIII581-VIII586.

20. Kurose, Y. (1987) "Recent Studies on Reinforced Concrete Beam-Column Joints in Japan," PMFSEL Rept. No. 87-8, Phil M. Ferguson Structural Engineering Laboratory, Univ. of Texas, Austin, 164 pp.

21. Yongchun, C., Guomei, C. and Hongqi, G. (1987) "Full Scale Tests on Seismic Behavior on Internal Reinforced Concrete Beam-Column Joints under Bidirectional Cyclic Loading," Inst. of Bldg. Struc., China Academy of Bldg. Res., Beijing, China,

July 1987.

22. Bolong, Z., and Yuzhou, C., "Behavior of Exterior Reinforced Concrete Beam-Column Joints Subjected to Bi-Directional Cyclic Loading," US-NZ-Japan-China Seminar report, Christchurch, New Zealand, August 1987.

23. Shahrooz, B. M., and Moehle, J. P., "Experimental Study of Seismic Response of RC Setback Buildings," Report No. UCB/EERC-87/16, Earthquake Engineering Research Center, University of California at Berkeley, October 1987, 347 pp.

24. Qi, X., "The Behavior of a RC Slab-Beam-Column Subassemblage Under Lateral Load Reversals," CE299 Report, Structural Engineering, Mechanics and Materials, Department of Civil Engineering, University of California at Berkeley, 1986.

25. Pantazopoulou, S. J., and Moehle, J. P., "Truss Model for 3-D Behavior of RC Exterior Connections," Journal of Structural Engineering, ASCE, Vol. 116, No. 2, February 1990, 298-315.

26. Velez, O. and French, C. W. (1989) "R/C Beam-Column-Slab Subassemblages Subjected to Lateral Loads," J. Struc. Engrg., ASCE, 115(6), 1289-1308.

27. Ammerman, O. V., and French, C. W. (1988) "Reinforced Concrete Slab-Beam-Column Connections," Struc. Engrg. Report No. 88-03, Dept. of Civ. and Min. Engrg., Univ. of Minnesota, 209 pp.

28. Pantazopoulou, S. J., Moehle, J. P. and Shahrooz, B. M. (1988) "Simple Analytical Model for T-Beams in Flexure," J. Struc. Engrg., ASCE, 114(7), 1507-1523.

29. Pantazopoulou, S. J., and Moehle, J. P., "Identification of the Effect of Slabs on Flexural Behavior of Beams," Journal of Engineering Mechanics, ASCE, Vol. 116, No. 1, January 1990, 91-106.

30. Yoshimura, M. and Kurose, Y. (1985) "Inelastic Behavior of the Building," ACI SP 84-7, Earthquake Effects on RC Structures: U.S. Japan Research, 163-201.

31. Tentative Provisions for the Development of Seismic Regulations for Buildings. (ATC 3-06). (1978). App. Tech. Council in Assoc. with SEAOC, Palo Alto, Calif.

32. Corley, W. G., "Rotational Capacity of Reinforced Concrete Beams," Journal of the Structural Division, ASCE, Vol. 92, No. ST5, October 1966, 121-146.

33. Schultz, A., E. (1990) "Experiments on Seismic Performance of RC Frames with Hinging Columns," J. Struc. Engrg., ASCE, 116(1), 125-145.

TABLE--1. Details and Strengths of Isolated Interior Connections

	Specimen Number						
	1 EW1 [9]	2 EW2 [9]	3 EW3 [9]	4 TIP [4]	5 TIM [4]	6 UTO [4]	7 J1 [15]
Geometry							
l1	120.0	120.0	120.0	192.0	192.0	106.3	204.0
l2	113.0	113.0	113.0	157.5	157.5	96.0	204.0
b_w	6.0	6.0	6.0	11.8	11.8	7.9	16.0
h	10.0	10.0	10.0	19.7	19.7	11.8	20.0
b_{trans}	10.0	6.0	6.0	11.8	11.8	7.9	20.0
h_{trans}	2.5	6.0	10.0	17.7	17.7	11.8	5.0
t_f	2.5	2.5	2.5	4.7	4.7	2.8	5.0
A_s	0.33	0.33	0.33	1.32	3.00	0.84	3.16
A_s'	0.22	0.22	0.22	0.88	1.80	0.84	2.40
A_{s1}''	1.51	1.51	1.51	1.26	1.26	0.54	2.81
A_{s2}''	0.00	0.00	0.00	2.55	2.55	0.00	0.00
b_1	113.0	113.0	113.0	66.9	66.9	96.0	204.0
b_2	0.0	0.0	0.0	90.6	90.6	0.0	0.0
d	8.7	8.7	8.7	17.5	17.4	10.6	16.6
d'	1.3	1.3	1.3	2.3	2.3	1.2	2.8
d"	8.8	8.8	8.8	17.4	17.4	10.4	18.0
Materials							
f_y	73.1	73.1	73.1	61.0	75.0	51.0	67.2
f_y'	73.1	73.1	73.1	61.0	75.0	51.0	65.6
f_y''	61.1	61.1	61.1	58.0	75.0	48.0	80.8
f'_c	5.5	5.8	8.0	4.9	4.0	2.7	3.5
Measured							
$M_{0.02}$	400	430	500	3270	4870	625	4120
Calculated							
M_{web}	246	247	252	1652	4220	517	3822
M_{ACI}	426	428	439	2393	5018	573	4526
M_{web+3h}	469	472	485	2889	5516	624	4999

TABLE--1. (Continued)

	Specimen Number					
	8	9	10	11	12	13
	J2	1D-I	2D-I	J3	K1	K2
	[15]	[18]	[18]	[21]	[20]	[20]
Geometry						
l1	204.0	160.0	160.0	169.0	106.0	106.0
l2	204.0	145.0	144.0	169.0	96.0	96.0
b_w	16.0	15.8	15.8	13.8	7.9	7.9
h	20.0	21.7	21.7	21.7	11.8	11.8
b_{trans}	16.0	23.6	15.8	13.8	7.9	7.9
h_{trans}	20.0	3.9	22.6	21.7	11.2	11.2
t_f	5.0	3.9	5.1	5.1	2.8	2.8
A_s	4.74	3.78	3.78	4.04	0.82	0.85
A_s'	2.64	2.37	2.37	2.15	0.62	0.61
A_{s1}''	2.81	1.28	3.71	6.01	0.59	0.59
A_{s2}''	0.00	0.00	0.00	0.00	0.00	0.00
b_1	204.0	145.0	144.0	169.0	96.0	96.0
b_2	0.0	0.0	0.0	0.0	0.0	0.0
d	16.7	19.2	19.2	19.4	10.0	9.7
d'	4.1	2.0	2.0	1.6	1.2	1.2
d"	18.0	19.7	19.7	19.1	10.7	10.8
Materials						
f_y	67.2	41.6	41.6	57.0	62.9	63.4
f_y'	74.2	42.1	42.1	56.9	62.9	63.4
f_y''	80.8	47.3	47.3	40.0	57.0	57.0
f'_c	4.0	5.5	5.4	5.4	3.5	3.5
Measured						
$M_{0.02}$	5560	4230	4490	7422	659	716
Calculated						
M_{web}	5387	3532	3528	5131	584	585
M_{ACI}	5991	3753	4173	5953	658	660
M_{web+3h}	6402	4125	5242	6965	723	727

TABLE--2. Details and Strengths of Isolated Exterior Connections

	Specimen Number						
	21 TEP [4]	22 TEM [4]	23 J3 [15]	24 2D-E [18]	25 J6 [22]	26 K3 [19]	27 GBS1 [20]
Geometry							
l1	200.0	200.0	204.0	160.0	169.0	106.0	78.7
l2	157.5	157.5	204.0	144.0	169.0	96.0	76.8
b_w	11.8	11.8	16.0	15.8	13.8	7.9	6.9
h	19.7	19.7	20.0	21.7	21.7	11.8	9.8
b_{trans}	11.8	11.8	16.0	11.8	13.8	7.9	6.3
h_{trans}	17.7	17.7	20.0	22.6	21.7	11.2	9.8
t_f	4.7	4.7	5.0	5.1	5.1	2.8	2.4
A_s	1.32	3.00	5.00	3.78	4.56	0.85	1.06
A_s'	0.88	1.80	3.16	2.37	2.36	0.61	0.82
A_{s1}''	1.26	1.26	2.81	3.56	5.97	0.59	0.50
A_{s2}''	2.55	2.55	0.00	0.00	2.55	0.00	0.00
b_1	66.9	66.9	204.0	144.0	169.0	96.0	66.9
b_2	90.6	90.6	0.0	0.0	0.0	0.0	0.0
d	17.5	17.4	15.8	19.2	20.3	9.7	8.0
d'	2.3	2.3	2.5	2.0	1.6	1.2	1.2
d"	17.4	17.4	17.5	19.1	19.1	11.0	9.3
Materials							
f_y	61.0	75.0	66.6	41.6	52.0	64.0	55.7
f_y'	61.0	75.0	67.2	42.1	56.3	64.0	55.7
f_y''	58.0	75.0	80.8	47.3	54.5	58.0	54.2
f'_c	4.7	4.9	4.7	6.9	5.3	2.9	5.5
Measured							
$M_{0.02}$	2410	4610	6250	4147	6511	745	645
Calculated							
M_{web}	1648	4288	5630	3568	5558	584	527
M_{ACI}	2428	5176	6276	4179	6663	661	577
M_{web+3h}	2881	5671	6733	5190	8001	728	641

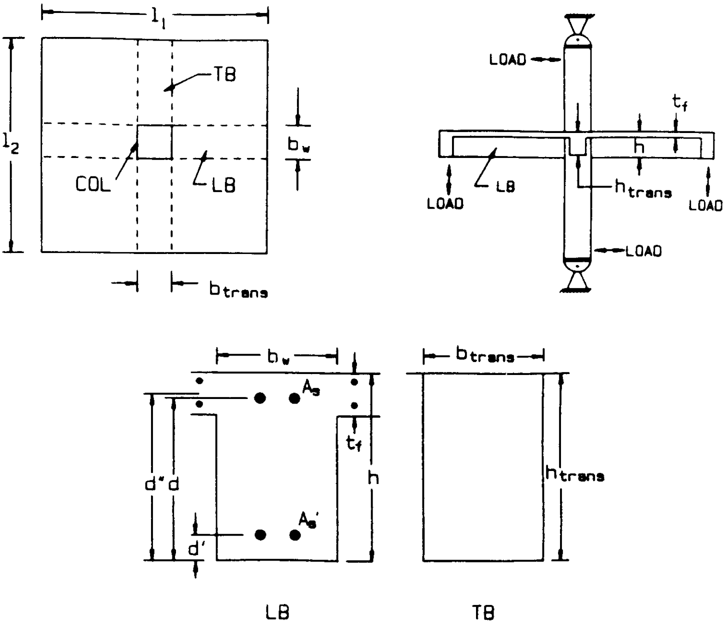

Fig. 1--Typical beam-column-slab test subassemblage

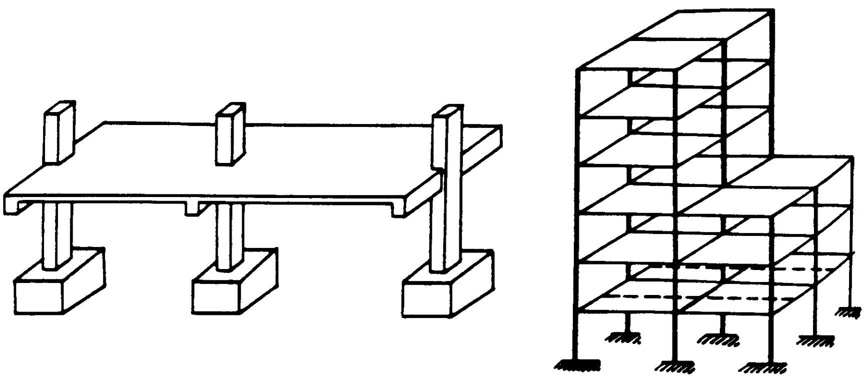

a) General view of the specimen

b) Six-story prototype model

Fig. 2--UCB two-bay test subassemblage (23-25)

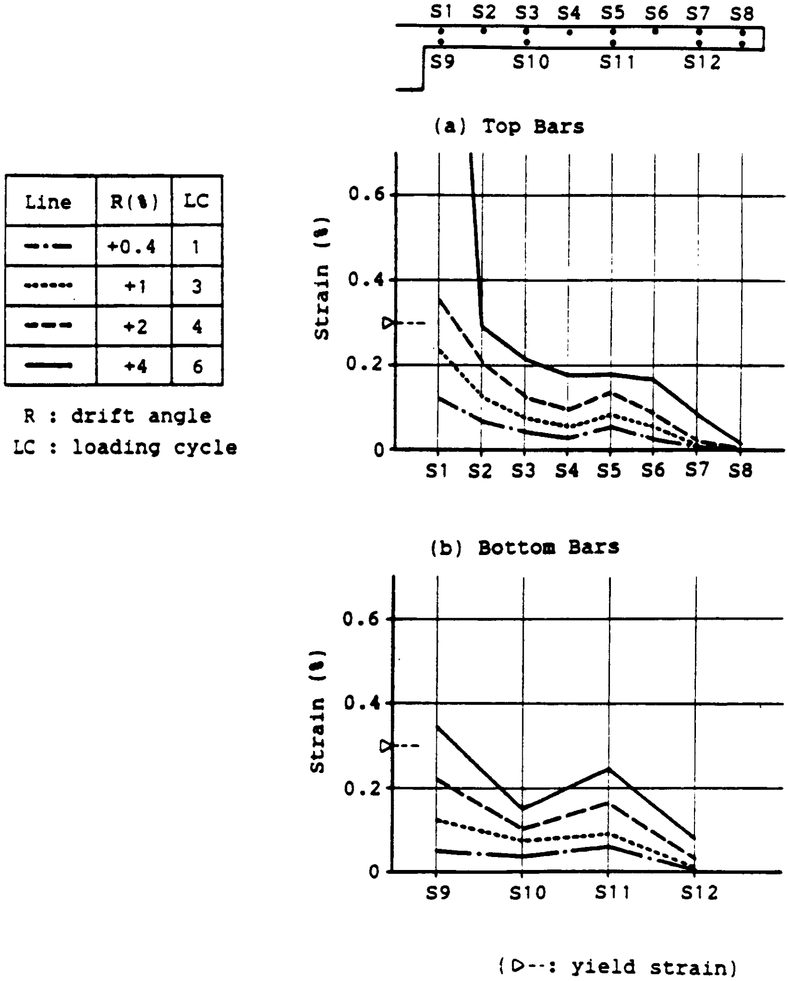

Slab Bar Strains in Negative Bending (Specimen J1)

Fig. 3--Strain distribution in longitudinal slab reinforcement measured along transverse beam line (15)

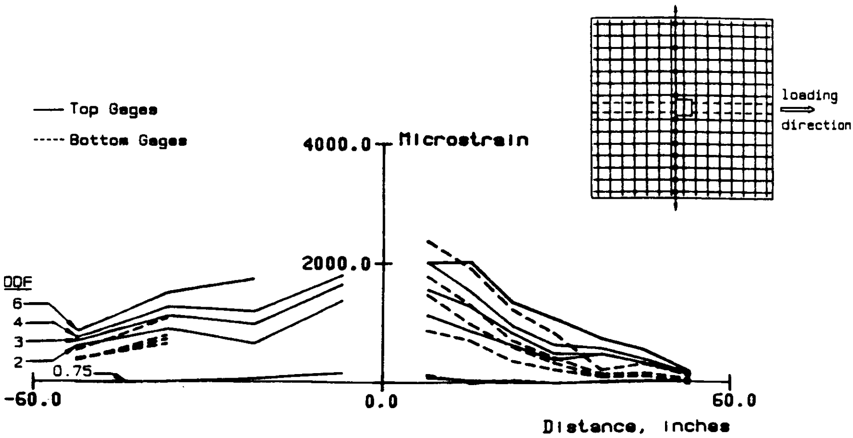

a) EW1 -- no transverse beam

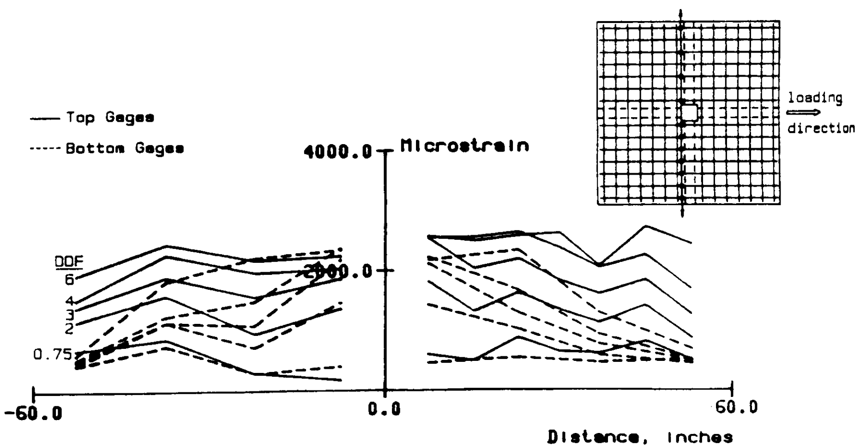

b) EW3 -- transverse beam

Fig. 4--Strain distribution in longitudinal slab reinforcement measured along transverse direction (10)

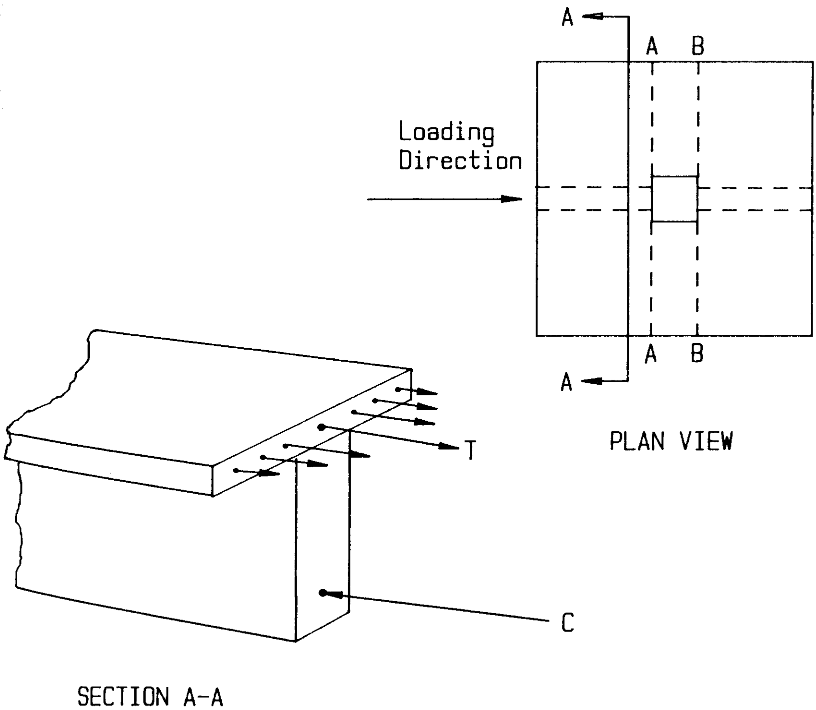

Fig. 5--Free-body diagram cut transverse to longitudinal beam line

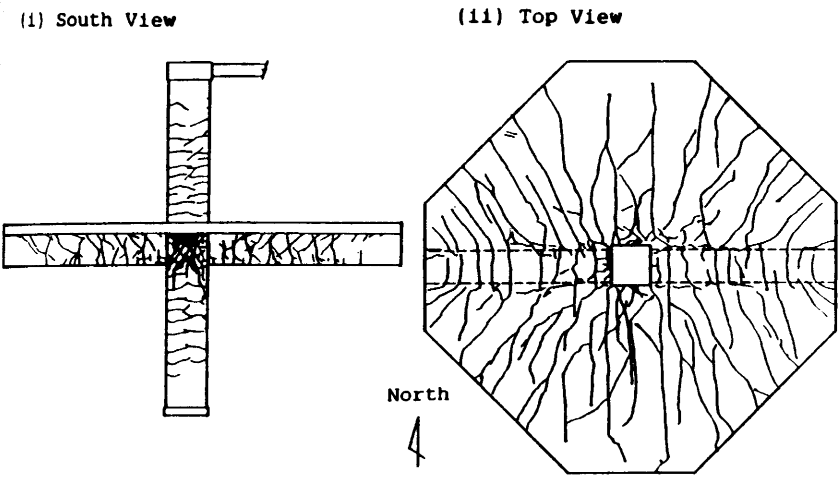

Fig. 6--Final crack patterns observed for specimen J1 (15)

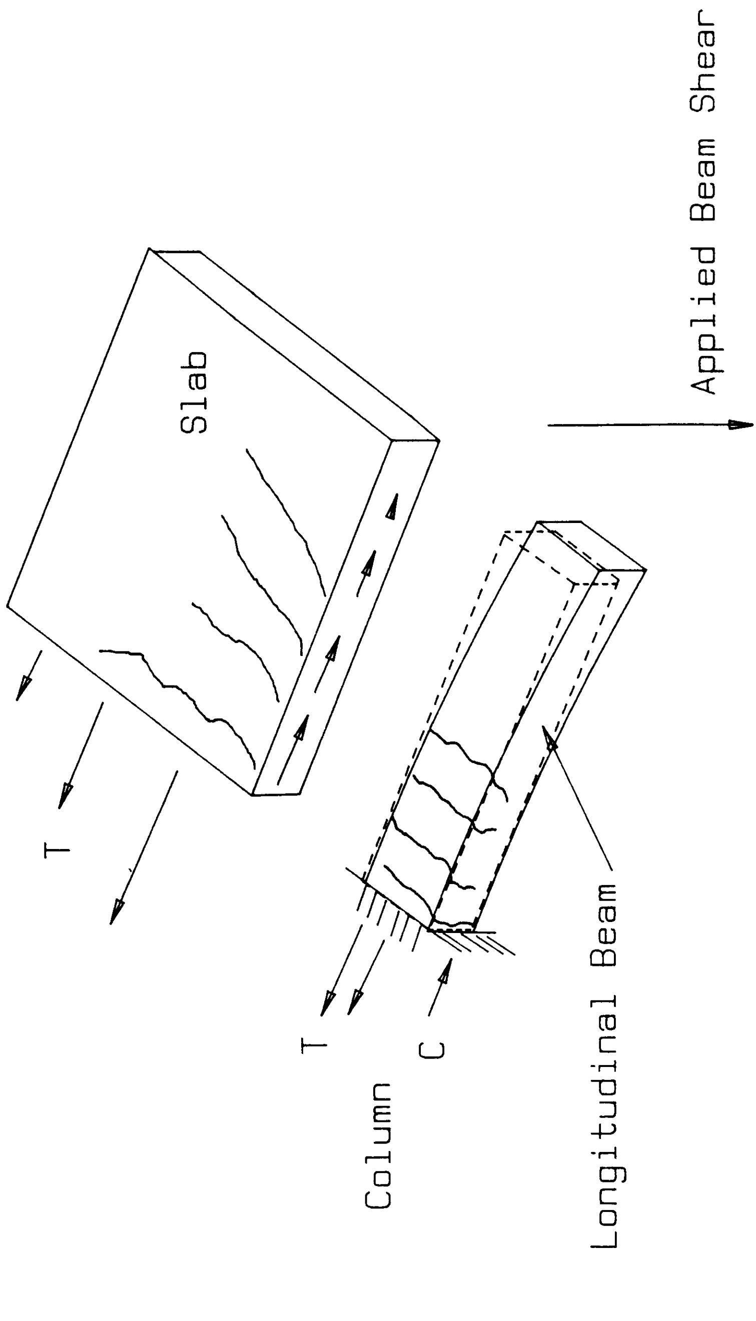

Fig. 7--Force transfer from longitudinal beam to slab

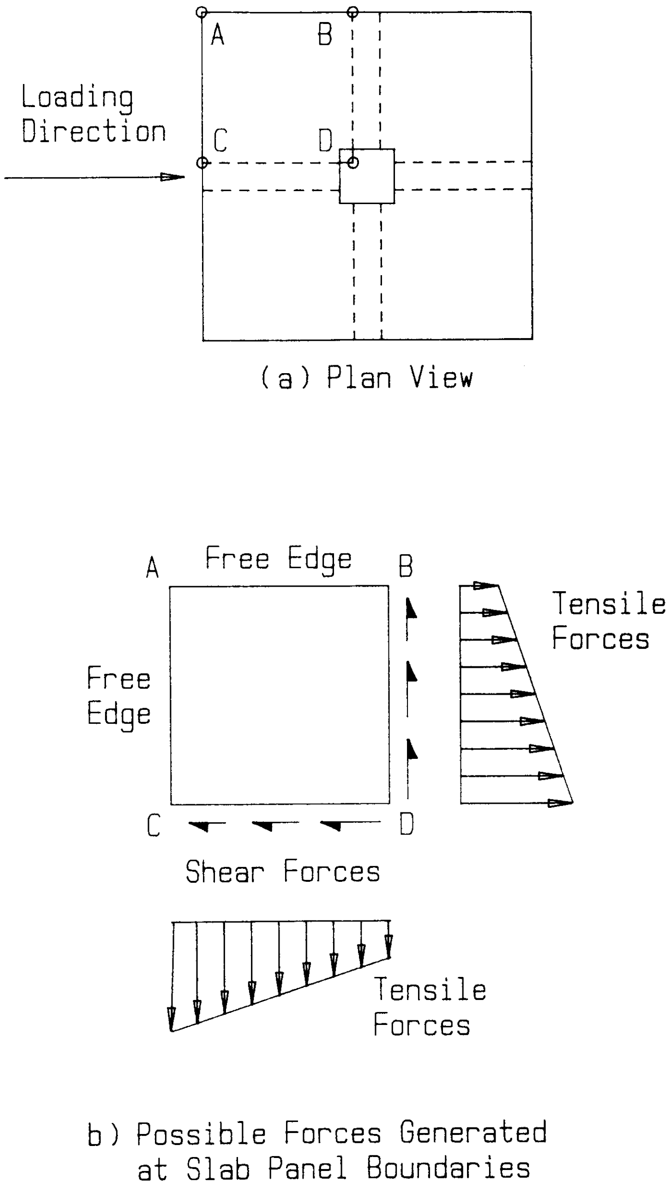

Fig. 8--Development of tensile forces in transverse slab reinforcement measured along longitudinal beam line

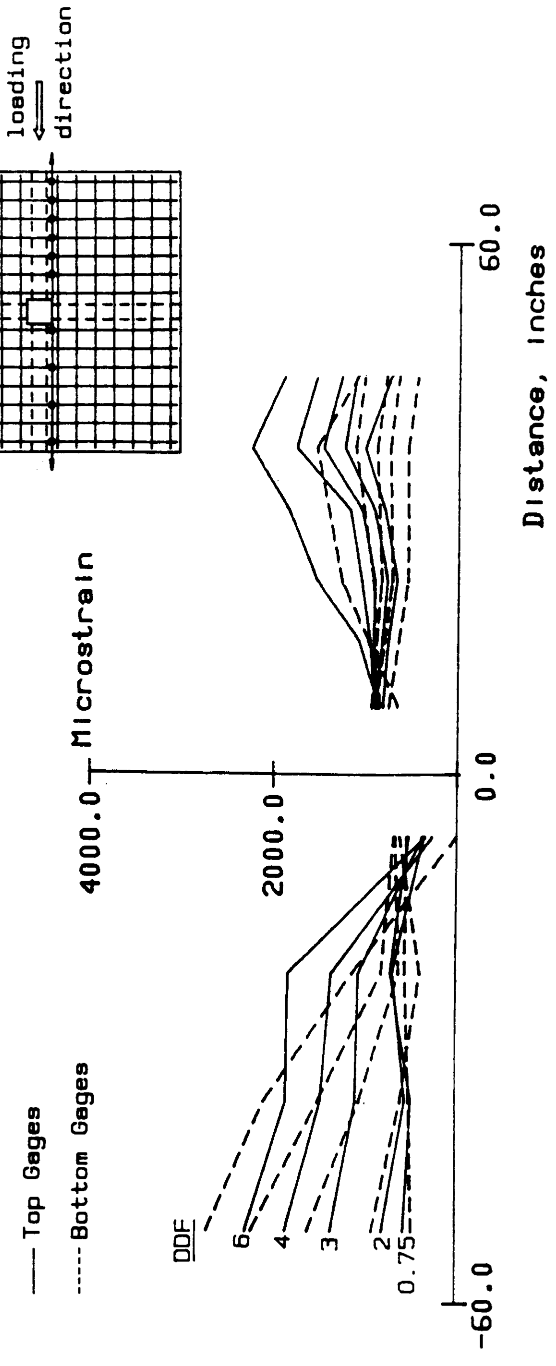

Fig. 9--Strain distribution in transverse slab reinforcement measured along longitudinal beam line for EW3 (10)

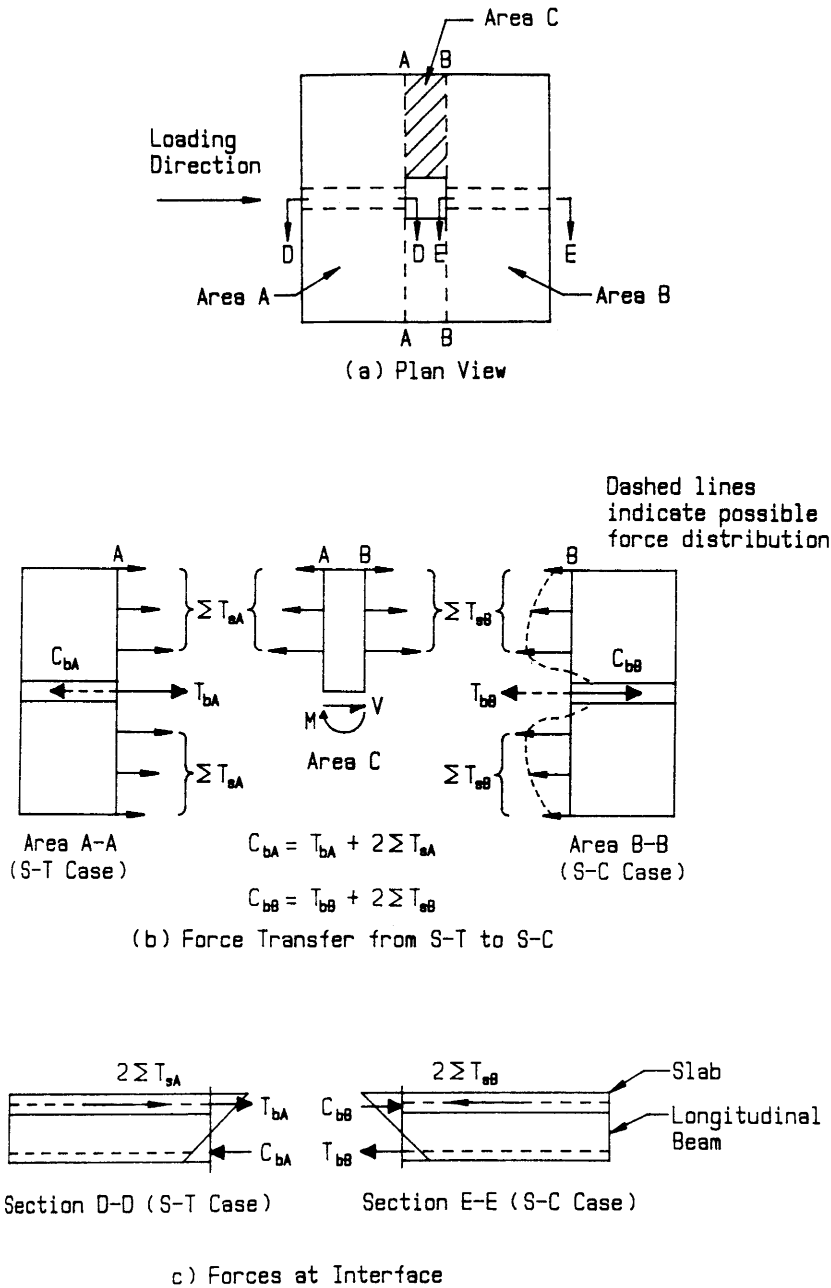

Fig. 10--Force transfer mechanisms across the slab

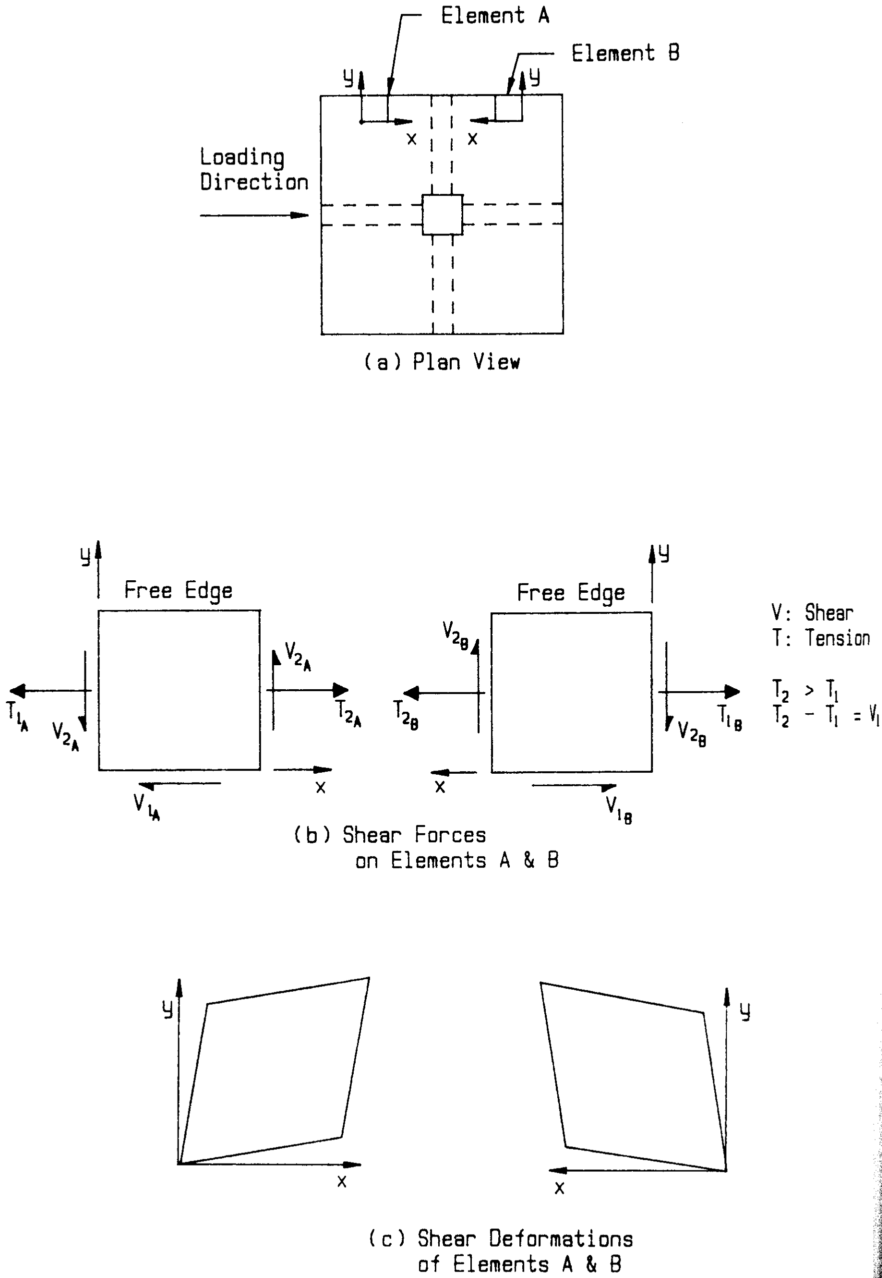

Fig. 11--Shear deformations of slab panels

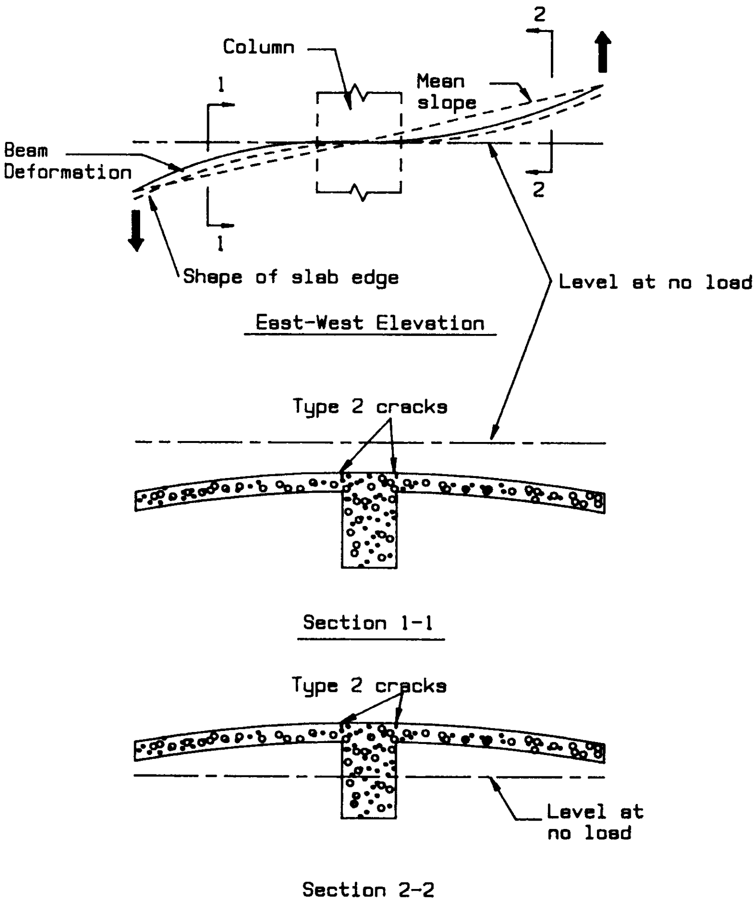

Fig. 12--Slab deformation relative to the longitudinal beam along subassemblage edge (18)

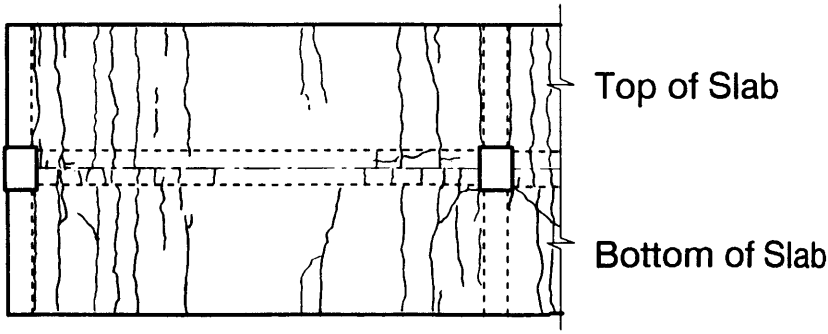

a) Continuous subassemblage, uniaxial loading 23-25

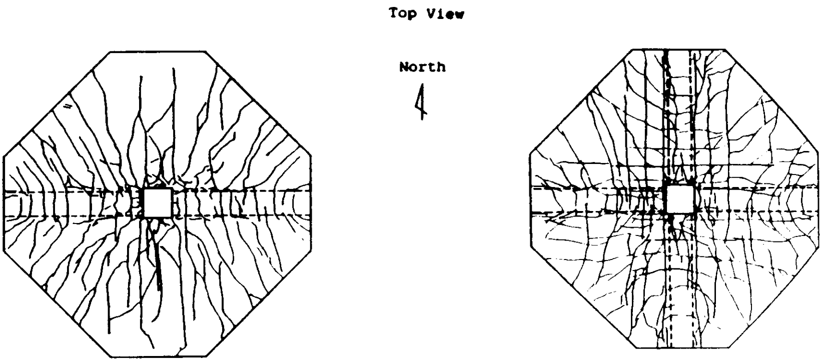

Final crack patterns for specimen J1

Final crack patterns for specimen J2

b) Isolated subassemblage, uniaxial loading (15)

c) Isolated subassemblage, biaxial loading (15)

Fig. 13--Crack patterns for continuous and isolated subassemblages

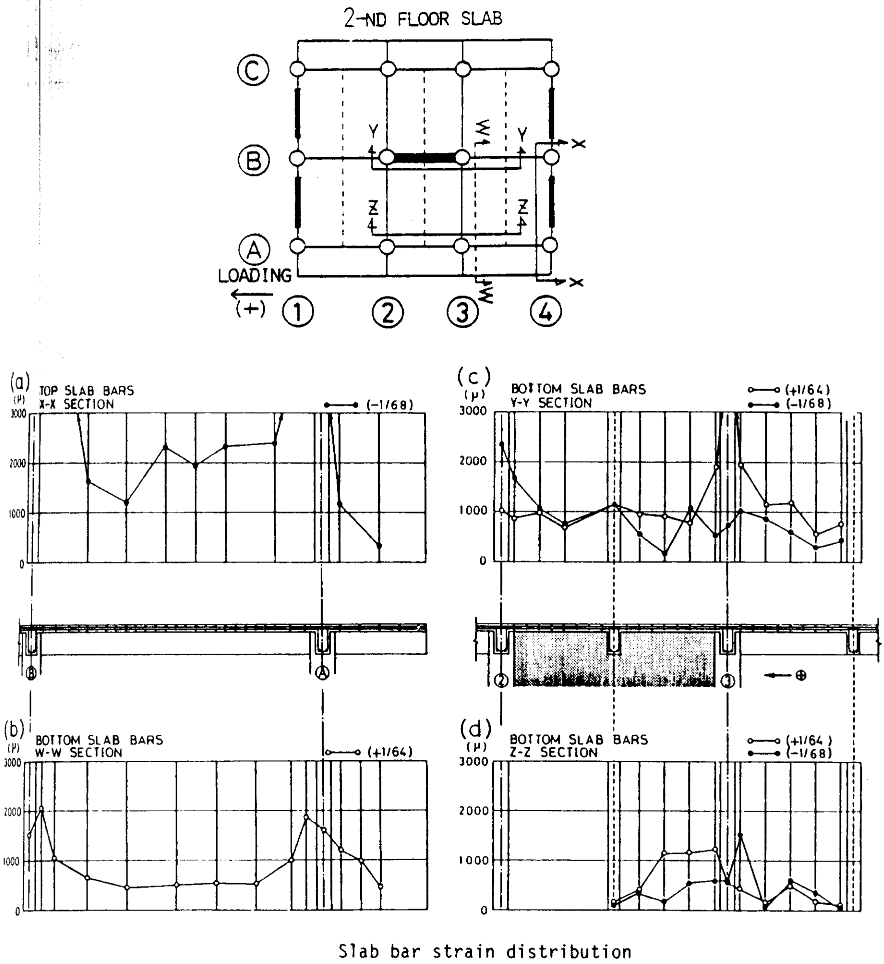

Fig. 14--Strain distribution measured parallel and perpendicular to loading in BRI structure (30)

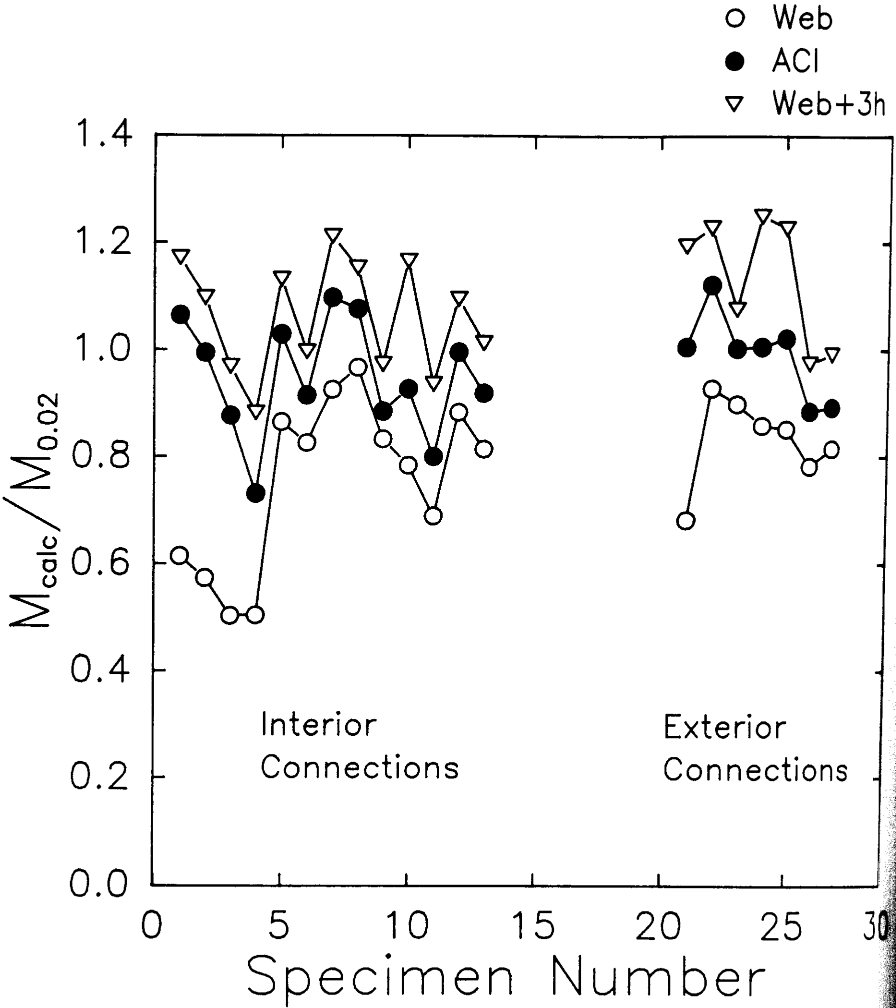

Fig. 15--Ratio of calculated flexural capacity (assuming various effective width assumptions) to flexural capacity measured at 2% interstory drift for specimens of Tables 1 and 2